2011 IEEE International Conference on Control Applications (CCA)
Part of 2011 IEEE Multi-Conference on Systems and Control
Denver, CO, USA. September 28-30, 2011

Radar-Based Detection and Identification for Miniature Air Vehicles

Allistair Moses†, Matthew J. Rutherford‡, Kimon P. Valavanis†

Abstract— **It is claimed that Unmanned Aerial Vehicles (UAVs) used for civilian/public domain applications will be dominant in the near future. Compared to UAVs used by the military, civilian UAVs are often operated by pilots without formal training, and hence they require increased levels of autonomy and intelligence, especially with regard to reducing threats to public safety. UAV integration into the National Air Space will require that the UAVs support multiple, complementary sense-and-avoid mechanisms, including detection and identification of other UAV-sized targets. Currently, the majority of available sensors are based on infrared detectors, focal plane arrays, optical and ultrasonic rangefinders. These sensors are generally not able to detect or identify other UAV-sized targets and, when detection is possible, considerable computational power may be required for successful identification. By contrast, this paper describes the design of a light weight, X-Band (10.5GHz) radar system for use on a small-scale (< 25 kg) rotorcraft. The prototype radar implementation is small enough to be carried by any miniature UAV, and it is capable of differentiating other miniature rotorcraft by their doppler signature. In addition to the overall hardware and software design of the prototype system, a performance analysis of various signature matching algorithms is presented demonstrating the capabilities of the system in a laboratory setting.**

I. INTRODUCTION

Unmanned aerial vehicles (UAVs) are becoming attractive solutions for non-military applications such as: traffic monitoring, fire protection, border patrol, among many others [1]. UAVs used by the military are generally powerful enough to carry advanced avionics equipment similar to that used in manned vehicles, are typically piloted by a team of highly trained individuals, and require a significant capital investment to operate. Civilian applications, however, are trending towards the use of smaller systems (i.e., Maximum Take-Off Weight (MTOW) $< 20kg$) operated by individuals or small teams with little formal training.

The development and implementation of an effective collision mitigation system is justified by analysis of the damage that can be inflicted by a collision event. For example, a collision between a 2kg UAV and a Learjet XR40 (traveling at cruising velocity) has a kinetic energy of approximately 57kJ. This is comparable to the 54kJ transferred by the impact of a 20mm anti-aircraft cannon shell [2], [3]. For lightweight vehicles (fabricated from compliant materials), a collision event is comparable with the collision between a bird and an aircraft. As birdstrike events are fairly common, modern jet aircraft are designed to withstand collisions between the airframe and 1.8kg to 3.6kg birds while traveling at 250kts with an altitude less than 10,000ft MSL [4]. However, many UAVs are constructed of composites, metals, and other rigid materials that are far less compliant than flesh and bone. Furthermore, there are a large number of UAVs with an MTOW greater than 3.6kg and are therefore capable of causing fatal damage to manned aircraft.

Overall, UAV integration into the National Air Space (NAS) will require multiple, complementary sense-and-avoid mechanisms (e.g., both vision- and radar-based systems). Therefore, it is critical that sensors be developed that are (1) suitable for small UAV integration (i.e, low weight), (2) sensitive enough to *detect* other UAV-sized vehicles, and (3) intelligent enough to *identify* and differentiate between different vehicle classes.

Cameras and other optical systems are often adversely affected by changing sunlight conditions and other environmental factors (e.g., smoke, fog, dust), limiting their ability to detect other vehicles. Furthermore, when detection is possible, identification and differentiation using such systems tends to be computationally intensive as the optical signals must be processed extensively to derive target type information.

We believe a solution to these problems can be found by utilizing a miniature radar system to perform both target detection and identification. While miniature airborne radar systems have been fielded before, the system described herein is unique in that it is designed to address the airborne sense-and-avoid problem, not act as a Synthetic Aperture Radar (SAR) imager or radar altimeter. Therefore, this paper describes the design and implementation of a lightweight (230gram), X-band (10.5GHz), doppler radar system suitable for use on commercially available, unmanned aerial systems.

A. Motivating Scenario

Within the realm of manned, commercial aircraft, mid-air collisions are mitigated by the Traffic Collision Avoidance System (TCAS) [5]. TCAS functions by means of on-board RF transponders and cockpit instruments that direct the pilot to make altitude changes to avoid a collision. While this system is effective, the use of the most basic TCAS systems is not required for piston engine aircraft with fewer than 10 seats. However, this class of aircraft composes a significant percentage of the world's aircraft. Further complicating the matter is the fact that most unmanned systems are not equipped with the TCAS system. If, however, the unmanned systems that must co-exist with general aviation aircraft were equipped with simple radar systems, then a new option for improving safety would be available.

Enabling collision avoidance behaviors on UAVs with low-cost hardware will provide relatively seamless integration

†Department of Electrical and Computer Engineering, ‡Department of Computer Science, University of Denver, Denver, CO 80208, {firstname.lastname}@du.edu

into the National Airspace System (NAS). The solution will be seamless in that when a collision course between a manned and an unmanned vehicle is detected, the manned vehicle will automatically be given priority and the unmanned vehicle will automatically perform a collision avoidance maneuver. This approach can be justified by noting that manned aircraft typically are incapable of the rapid, sustained high-g, maneuvers some UAVs can perform. Moreover, an automated system is capable of continuous monitoring throughout the entire flight regardless of operator workload or mental state.

For example, consider a radar-equipped miniature unmanned rotorcraft sharing the airspace with a Cessna 172R manned aircraft [6]. The unmanned rotorcraft (based on an Align TRex450Pro helicopter) rotorcraft has a typical flying weight of 0.75kg and a maximum thrust of 1.1kg (10.78N) measured at 1600m above sea level. As TCAS avoidance maneuvers are altitude changes, the maximum vertical dimension of the Cessna must be considered, for the Cessna 172R this dimension is 2.72m. To cover this vertical distance, the rotorcraft would require no more than 0.624 seconds to evade the manned aircraft. The Cessna's cruising speed of 140mph (62.6m/s) is typical of small single piston engine craft, and at this velocity, the manned aircraft would have covered approximately 39m. This provides an estimate of the minimum required radar detection/identification range. Assuming a maximum range of 500m against a Cessna 172R-sized target and a 1Hz update rate, the altitude separation factor of safety is 125 (i.e., the unmanned rotorcraft equipped with such a system could cover 125 times the distance required to avoid a collision with any part of the Cessna).

The remainder of this document is organized as follows: Section II provides background on radar systems and Section III presents related radar-based sensor work. In Section IV, we describe the hardware and software design of our system. We describe target data processing in Section V and the results of our evaluation in Section VI. Finally, Section VII concludes.

II. BACKGROUND

Radio detection and ranging (RADAR) utilizes electromagnetic energy (typically in the microwave range) to gather information on remote objects by analyzing the characteristics of their reflected energy. Most large scale radar installations utilize some form of pulsed radar arrangement to extract information about the targets by timing the radar returns. However, the complexity, limited range resolution, and large minimum range of pulsed radar systems preclude their adoption for miniature UAV applications. These issues are resolved through the use of Continuous Wave (CW) radars. CW radar systems can be divided into two generalized forms: Frequency Modulated Continuous Wave radar (FMCW), and Doppler radar. The former utilizes periodic variations in frequency to determine the range to the target while the latter relies on the Doppler Effect to isolate moving targets and determine their velocities relative to the radar antenna, but it is incapable of determining the range to the target. While the hardware described in this paper is capable of both FMCW and Doppler operation, only the Doppler operation mode is utilized in our current prototype. A practical system will typically operate in doppler mode until a target is detected. Once the presence of a target has been detected, FMCW mode will be activated to provide range data to the target. In this fashion, the false alarm rate can be kept low by only responding to targets with some radial velocity relative to the RADAR. Furthermore, the overall reaction time is decreased by the use of Doppler mode since a target's presence and velocity can be acquired from a single sample window, whereas FMCW must use multiple sample windows to determine the velocity based on the differentiated ranges.

$$\triangle F = F_t(\frac{2v}{c-v}) \tag{1}$$

$$\triangle F = 70.048v \tag{2}$$

At the heart of Doppler radar operation is the Doppler frequency shift generated by some combination of moving sources, and/or targets. For co-located transmit and receive antennas, Equation 1 defines the Doppler shift as a function of the target velocity relative to the transmit antenna **v**, the transmitted frequency $\mathbf{F_t}$ and the speed of light **c**. Analysis of Equation 1 reveals that for low velocity targets, Equation 1 can be simplified into Equation 2 given $\mathbf{F_t} = 10.5GHz$. Utilizing this information, the velocity of various targets can be determined by measuring the frequency shift.

For advanced UAV-based control applications, it is necessary to both determine target velocity and to identify the target in question. As most air vehicles, while in operation, primarily consist of rotating components moving in a periodic manner, there exists a unique Doppler signature for most vehicles. *A priori* knowledge of this signature can be utilized in realtime to determine the presence of a familiar target vehicle within the currently imaged scene. For example, the Align TRex-450Pro helicopter doppler signature can be expressed as having frequency peaks described by Equation 3.

$$S_{Heli} = (\frac{2F\pi}{CT})[d_{mr} + d_p + \frac{d_{tr}}{1/4.24}] + Aux(T) \tag{3}$$

Where $\mathbf{d_{mr}}, \mathbf{d_p}$, and $\mathbf{d_{tr}}$ are the diameters of the main rotor, paddles, and tail rotor, respectively. Note the scaling factor 4.24 applied to the tail rotor frequency component. This is due to the gear ratio between the main and tail rotors. $\mathbf{F_t}$ is the transmit frequency, **c** is the speed of light, and **T** is the rotational period of the rotor system. **Aux(T)** represents additional components within the helicopter (the motor, main and tail rotor transmissions, drive shafts, etc). Essentially, the model is a representation of the velocities caused by the moving vehicle components. As each vehicle class is described by different model, the quantity and location of frequency peaks act as a "fingerprint" for vehicles of the class. Although Equation 3 assumes the velocity of a rotating part is concentrated at a single point, when in practice it is distributed over the length of the part, the actual signatures

observed in practice are different enough that identification is still possible, as depicted in Figure 7.

III. RELATED WORK

The use of radar systems for determining the type (and often the model) of vehicle(s) within the current scene is not new. This functionality has been present in larger vehicles and installations including most modern military aircraft and airport installations. The level of detail possible is readily demonstrated by the U.S. Army Research Laboratory [7], and other research groups [8], [9], [10], [11]. For large-scale vehicles, and especially in the case of turbine powered systems, identification is eased by the possibility of sensing not only the larger aerodynamic components, but also the doppler modulation caused by the power source. Indeed, Jet Engine Modulation is one of the foremost methods of target identification in the absence of large periodically rotation parts (e.g. a helicopter rotor system) or when attempting to identify a non-cooperative target. As demonstrated by these research groups, there exist numerous ways to identify targets of interest. However, the methods used by these groups typically involve the use of a parametric target model. This is suitable for full scale vehicles due to the small number of vehicle types and variants. However, on a typical miniature UAV scale (vehicles $< 25kg$), the number of possible variants is significantly greater. From a practical perspective, this implies that non-parametric models are preferable since the manual generation of a parametric model for every UAV variant is not feasible.

Additionally, even in the absence of large (with respect to the wavelength of the carrier) or complex structures (such as jet engine compressors), identification of UAV-scale vehicles is still possible, albeit at shorter ranges and higher frequencies. This is because the integral vehicle components of smaller vehicles modulate electromagnetic radiation in a manner comparable to large scale systems [12].

In addition to the capabilities of modern radar systems, there has also been significant progress with regard to miniaturization. Examples of such miniature UAV-capable radars are the BYU microSAR imager [13], imSAR's nanoSAR line [14], and Roke's MRA line of radar systems [15]. However, it should be noted that these radar systems function as Synthetic Aperture Radars, and in the case of the MRA, as a radar altimeter. In other words, these systems are designed for providing information on the terrain that the vehicle is flying over, and not the airborne obstacles the vehicle may run into. Furthermore, despite the great strides made by these systems, their high cost and high mass make them impractical for many miniature UAV applications.

IV. SYSTEM DESIGN

From inception through all phases of development, every component of our radar system has been designed such that it could be deployed on a wide variety of miniature aerial vehicles. Due to this requirement, a modular approach was selected to allow for the individual system components to be dispersed over the vehicle structure, thus, simplifying the vehicle mass distribution requirements. Indeed, virtually any UAV capable of supporting a payload as described in Table I can be equipped with this system. Furthermore, a variety of different module combinations can be selected to suit a range of applications and scenarios. This enables an optimized sensing solution to be rapidly developed for most UAV systems. For example, if a different transmit frequency is desired, only the RF section of the radar must be changed. Likewise, if the current antenna arrangement is not suited for a particular application, another antenna can be used since the RF section utilizes industry standard waveguide components.

System Mass	230 grams
System Dimensions	15.5, 10, 9 cm
Power Consumption	4.5 Watts
Input Voltage Range	10 to 42 VDC
Transmit Frequency	10.5 GHz
Transmit Power	10mW

TABLE I
SYSTEM SPECIFICATIONS

A. Hardware

The first module to be described is the RF front end module. The design of this component is crticital to the correct functioning of the system. Therefore, all efforts were made to utilize efficient technologies with a proven track record of success. The specific function of this module is to generate, transmit, receive, and finally down-convert the received signal for use in subsequent stages. Several architectures were investigated for this task. The first design iterations utilized PCB-mounted discrete components. However, these designs suffered from significant losses due to the high frequencies involved and the losses incurred when coupling the front end to the antenna system. These problems were solved in the current design iteration by utilizing a relatively common waveguide-based microwave device known as a Gunnplexer. The Gunnplexer consists of a Gunn diode mounted within a resonant cavity. Also located within the cavity are a ferromagnetic circulator and a mixing diode. The Gunn diode functions as a voltage-controlled microwave source. The microwave energy from the oscillator is then divided between the mixing diode and the antenna. The portion of the energy diverted to the mixing diode functions as the local oscillator signal which is mixed with the portion of energy reflected from the target. This mixing process (frequency domain multiplication) produces an output known as the Intermediate Frequency (defined as $\delta(F_L - F_T)$) in addition to other typically unwanted frequencies, see Equation 4. These unneeded frequencies are filtered at a later stage.

$$Output = \delta(F_L - F_T) + \delta(F_L + F_T) + \delta(nF_T) + \delta(nF_L) \quad (4)$$

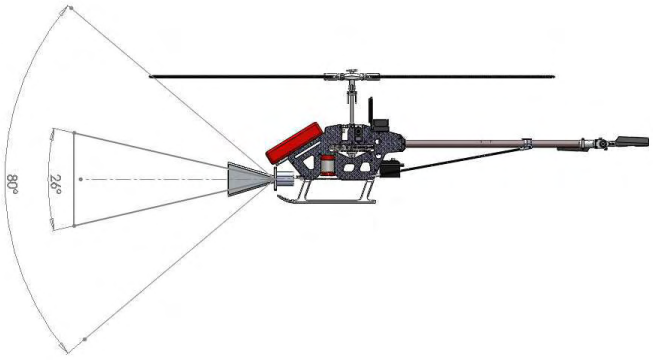

Fig. 1. Interaction between main lobe and carrying vehicle

The signals to and from the Gunnplexer are conveyed to and from the environment by means of an antenna whose primary function is to shape the electromagnetic radiation transmitted from the Gunnplexer, and to increase the range of the system by presenting a larger aperture to the return signals. During development, numerous antenna designs were evaluated including: helical, phased array patch, and parabolic. Evaluation, using software packages such as Antenna Magus, determined that a horn antenna is the simplest solution that would provide the best performance given the following constraints:

- **Low Mass**: As the system is destined for miniature UAV applications, overall system mass is a critical consideration. Horn antennas can be fabricated from nearly any material, provided a conductive coating thicker than the skin depth is deposited on the interior [16].
- **Simple Internal Structure**: Horn antenna designs can be fabricated from simple materials without depending on specific internal periodic structures as opposed to slotted waveguide arrays or phased array patch antennas.
- **High Gain & Directivity**: Horn antennas provide excellent gain characteristics, given their complexity.
- **Low Loss**: Direct coupling with the Gunnplexer assembly dramatically the lowers insertion loss, and thereby improves performance. Other designs typically require a waveguide to coaxial adapter in addition to other impedance matching structures within the antenna.

While the primary motivating force behind the antenna design is the performance of the radar system, the application environment is also of great importance. As this is a radar system designed for miniature UAV applications, the antenna, and the resulting radiation pattern, must be compatible with the carrying vehicle. For rotorcraft-based airborne target detection, identification, and avoidance applications, a forward-looking field-of-view is desired. This requirement places a restriction on the maximum main lobe angle, otherwise undesired noise will be introduced into the system as a result of interaction between the antenna main lobe and the vehicle propulsion system. Although some level of interaction is inevitable, every effort should be made to reduce this interaction. Figure 1 demonstrates this situation for miniature helicopters. The main lobe angle of the antenna discussed in this paper is approximately 26 degrees while the gain of the antenna is $>$ 17dBi.

After undergoing the frequency domain multiplication described above, inbound signals pass through the intermediate frequency amplifier (IF amp) module. The primary function of this module is to amplify the relatively weak signal resulting from the frequency down-conversion performed within the RF front end. Its secondary function is to filter the IF signal before and after each gain stage. This processing occurs in two stages. The first stage serves to present the mixing diode with a high impedance load and to attenuate undesirable signal characteristics. The first undesired characteristic is the input signal DC bias. This is caused both by imperfect isolation parameters within the Gunnplexer circulator as well as targets with no radial velocity. Both factors result in identical RF and LO frequencies which, after down-conversion, give rise to a DC voltage. The second unwanted signal is the high frequency (RF+LO) sum frequency. Following removal of these components, the signal voltage is amplified by the first gain stage ($gain = 11\frac{v}{v}$). Subsequent to the first gain stage, the signal is sent through a high pass filter to remove the DC offset generated by the first gain stage and remove low frequency interference (e.g., 60/50Hz mains frequencies, motor speed controllers, etc.) present within the signal. Finally, the signal is sent through the second gain stage ($gain = 6267\frac{v}{v}$) and is ready for digitization. The total voltage gain of the IF amplifier module is $68,937\frac{v}{v}$. This staged amplification process is essential to proper system operation. If amplification is performed in a single stage, the noise present within the intermediate frequency would saturate the amplifier output.

In order to further reduce the influence of noise on the system, the amplifier module is mounted directly on the Gunnplexer body. This reduces the length of conductor that carries the low voltage signal from the mixing diode. The complete, analog section of the radar system, when attached to the RF modules, increases the mass of the RF/analog section to 137 grams.

Once the signal has been received and amplified by the analog modules, it is digitized. This is performed by means of a 16-bit, 250ksps, analog digital converter (ADC) [17]. The Shannon-Nyquist theorem states that to accurately measure a signal without aliasing, one must sample the signal at twice the maximum frequency present within the signal. In our case we are sampling the IF signal, so application of doppler equation to equations (1) and (2), we learn that given our sampling frequency of 250ksps the maximum measurable frequency is 125ksps, which corresponds to a maximum measurable target velocity of 1784m/s. In practice, for most UAV applications, the need to track objects with this velocity will most likely never arise due to the relatively low cruising speeds typical of most UAVs. Thus, the ADC sample rate is

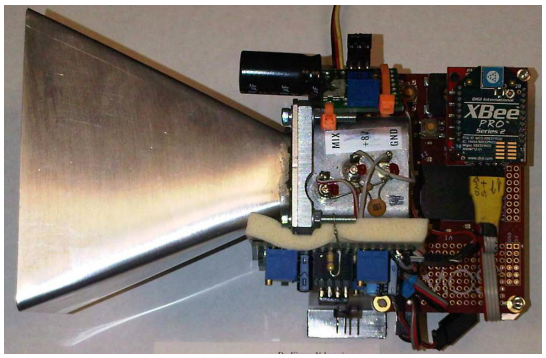

Fig. 2. Complete radar system

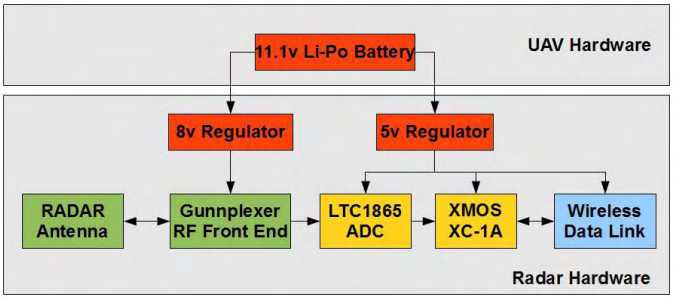

Fig. 3. RADAR System Hardware Diagram

varied to form a compromise between target velocity ranges, velocity resolution, and finally system memory limits. The varying sample rate is achieved by introducing a delay after each ADC sample. Upon sampling, all on-board processing is performed on a 1600MIPS, four core, multi-threaded, microprocessor (XMOS XS1-G4). The parallel processing enabled by this hardware is essential to achieving high performance levels in that it enables pipelining of data operations. It should be noted, however, that the system detection speed is limited by the need to decrease the sampling frequency to increase the frequency resolution, not by computational complexity.

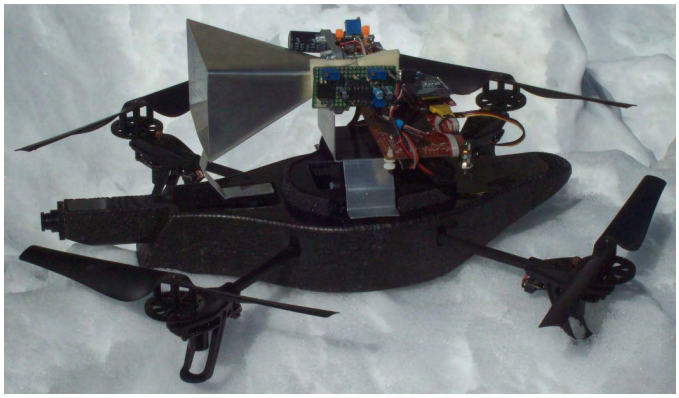

Fig. 4. MAV Equipped with radar system

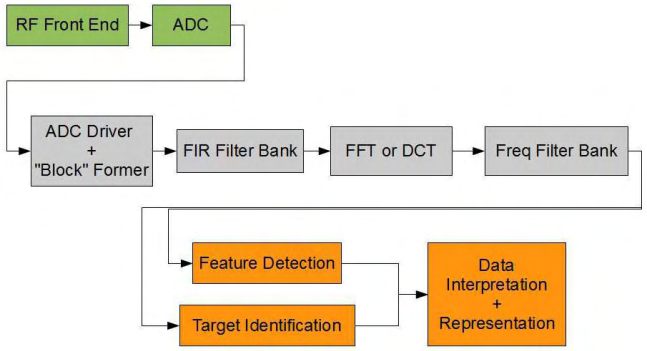

Fig. 5. Data pipeline overview

The complete radar system, see Figures 2 and 3, consists of the RF section, analog amplifier, signal processing boards, wireless telemetry, and mounting brackets and hardware. The overall systems specifications are displayed in Table I. Figure 4 displays the radar system being carried by a low-cost, commercially available quadrotor, the Parrot AR drone.

B. Software

The on-board processing software is composed of several discrete modules, see Figure 5. The architecture of the XMOS processor utilized allows software to be cleanly organized as different tasks with high-performance channels between them. In Figure 5, the first two (green) rectangles represent the hardware modules just described. The rectangles in the second row are implemented on the XMOS processor as tasks, with the arrows between them representing unidirectional data channels. The use of channels for inter-task communication obviates the need for sophisticated (and error prone) synchronization to protect shared global memory, and allows each task to perform blocking I/O on the ports / channels it is concerned with, again resulting in clean, well-organized software. Each module is executed, in parallel, as a distinct task. The in-hardware scheduler on the XMOS ensures that all tasks are scheduled fairly and with great regularity (round-robin among the active tasks for a single instruction). The “ADC Driver” module samples the ADC continuously and generates data packets that are forwarded to the other modules. The size of the data packets is variable as a function of the desired frequency resolution and velocity range – for our prototype a fixed size of 512 samples is used. The second module consists of a set of FIR filters. These filters serve to eliminate variable noise that was not attenuated by the IF amplifier module. This approach is particularly effective as digital filters can provide steep rolloff rates, and can be implemented within the DSP as dictated by application requirements. For example, if the UAV is operating near power lines, a 60Hz FIR notch filter can be introduced to enable successful operation. The third module consists of a Fast Fourier Transform (FFT) operation required to generate frequency domain information. The fourth module is an additional digital filter block used to filter the

frequency domain signal representation. This filtering is used to eliminate erroneous target information and increases the reliability and simplicity of subsequent processing blocks.

The result of these first four software modules depicted in Figure 5 is a 256-sample frequency-domain signature (we discard the "bottom" 256 samples from the FFT as they are simply a mirror of the ones we use). This signature is now ready for use in target detection and identification.

V. TARGET DATA PROCESSING

As depicted in Figure 5, target data processing can be divided into two generalized scenarios: point target detection and complex target identification. In the first scenario, the target(s) consist of a single object with either no or ignored internal structure. That is to say, the entire target object and all components can be considered to be traveling at the same velocity. In this mode identification is not possible, but target velocity is readily available.

Multiple targets can be detected and their velocities (relative to the Poynting vector) can be determined. However this functionality is limited by the velocity differences between the individual targets and the doppler-generated bandwidth occupied by the targets.

The second scenario is characterized by a target of suitable complexity within the radar main lobe. In this situation, a complex target is defined as having numerous periodically moving parts. High levels of complexity are required for reliable system operation.

A. Simple "point" targets

Target velocity information, for simple scenarios, can be determined by applying a smoothing filter (low-pass or median) to the raw FFT data then executing a peak finding algorithm to determine the main target velocity. Equation 2 can then be used to obtain the target velocity in m/s. This procedure is illustrated in Figure 6. The target utilized to generate the data in Figure 6 was a human walking directly toward the radar antenna.

Further analysis reveals the importance of the smoothing filter and a priori knowledge of the types of signals expected. The target in question, was swinging her arms while walking toward the antenna. Moreover, there were other additional sources of motion (e.g., clothing, legs, etc.) whose motion was not completely parallel to the main lobe Poynting (propagation) vector. This results in target spectral broadening. Since other targets tend to have similar movement patterns, a priori knowledge is needed to determine the type of post-processing required to extract the desired information. For example: multiple targets traveling at similar velocities (relative to the radar antenna) would have their individual signatures merged into a single average velocity after the filtering operation.

B. Complex targets

Targets assumed to be "complex" are evaluated in a different manner. This is due to the presence of a relatively predictable signal structure that enables target identification. The nature of the signals can be seen in Figure 7.

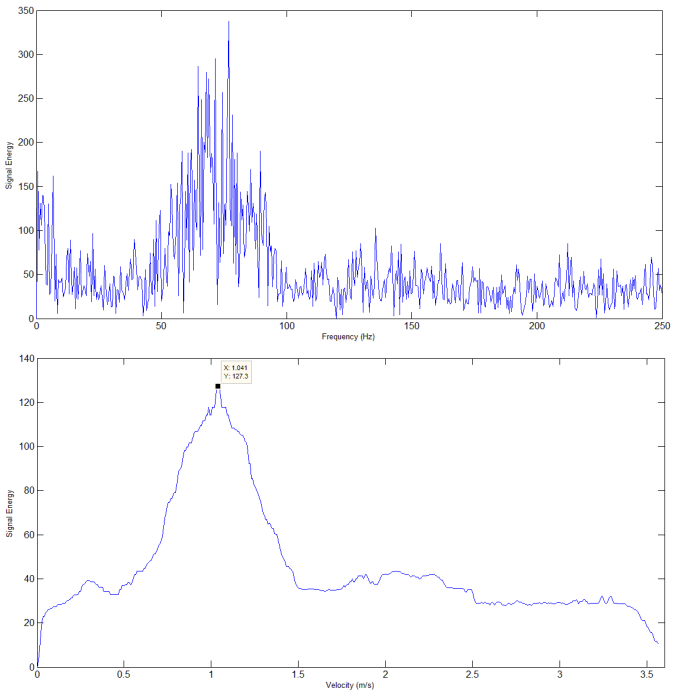

Fig. 6. Point target: walking human

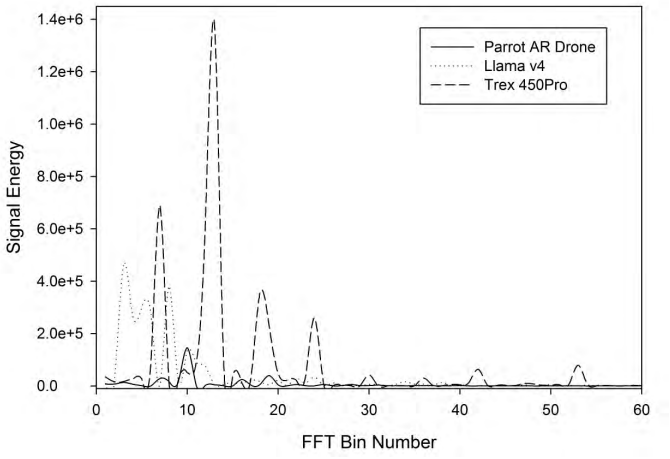

Fig. 7. Miniature Rotorcraft Signatures

Figure 7 displays the the instantaneous doppler frequencies of three miniature vehicles: a coaxial rotor helicopter (E-Sky Lama v4), a commercially available quadrotor (Parrot AR Drone[18]), and the TREX 450 Pro. When compared with the radar signature of a human, the rotorcraft exhibit a less complex signature.

Examination of Figure 7 shows the majority of signal energy is present in the lower frequencies. While the signals generated by the down-conversion process bear higher frequency components, these higher frequencies are filtered by the IF amplifier module leaving their lower frequency harmonics.

This characteristic of our system is advantageous in that

we can use it to determine the velocity of the target relative to the radar. We do this by reducing the number of samples that comprise a signature from 256, and sliding this truncated target signature along the 256-sample scene signature, determining the match quality at each point. If the best match occurs at a non-zero offset, then the target bears a radial velocity corresponding to the offset.

C. Target library

As described earlier, advanced control strategies for unmanned UAVs require both detection and identification. In order to detect the presence of a target of interest, we must be able to differentiate a given signature from the background scene within the range of the radar. In order to identify different targets, we must be able to determine that a given signature matches one of a database of pre-recorded signatures of vehicle classes of interest. Fundamentally, both of these operations involve comparing a given "live" signature, with a library of pre-recorded signatures and determining which is the best match. We represent both the background signature and vehicle signatures within this signature library, and are then able to perform detection and identification in the same computational step (i.e., if the live signature matches the background signature the best, then we know there is no target of interest within range).

VI. SYSTEM EVALUATION

During development, we implemented a simple user interface to the radar over a bi-directional serial link that enables it to operate in either data collection mode or target matching mode. We focus, now, on two different evaluation analyses. In the first, we utilize data collection mode to gather a large number of live samples of different vehicles in order to evaluate different matching algorithms off-line. The second evaluation performed is to determine whether the radar system can successfully implement the matching logic on board in a real-time scenario with live targets.

A. Matching Algorithms

As described above, the fundamental computational operation performed by the radar system is to match an incoming "live" signature against a library of pre-recorded vehicle signatures. In order to evaluate different algorithms efficiently, we utilize the data collection mode of the radar to record 160, 256-sample signatures for the three vehicles whose signatures are depicted in Figure 7, namely the coaxial helicopter, the Parrot AR Drone quadrotor, and the TREX 450 Pro helicopter.

For these experiments, the radar system and target vehicles are placed inside a reinforced concrete room. Throughout the experiments, the range between the radar system and target vehicles is fixed at 3 meters (10 feet). The linear separation distance between each vehicle was 0.6m resulting in an angular separation of 11.31° No effort was made to reduce or account for multi-path signals or reflections from the background. The vehicle signatures are recorded by fixing the vehicle to the floor of the test room and throttling the rotor system to typical flight speeds. The radar system is then pointed at the target vehicle and a series of signatures are streamed back to the attendant PC over the dedicated (wired) serial link; 160 of these signatures are gathered per vehicle and saved into a log file.

Due to the presence of noise in the signatures we experimented with averaging a varying number of raw signatures into a "library signature," using a simple arithmetic average per sample position. For example, when averaging 10 signatures, all 10 values in the first of 256 buckets is combined to give the average value for the first bucket. For each such library signature, we compare it to all other signatures created by averaging the same number of raw signals across the three vehicles. We perform identification by calculating the best match across all vehicles using the algorithms described below. If the best match comes from the correct vehicle, it is counted as a successful match.

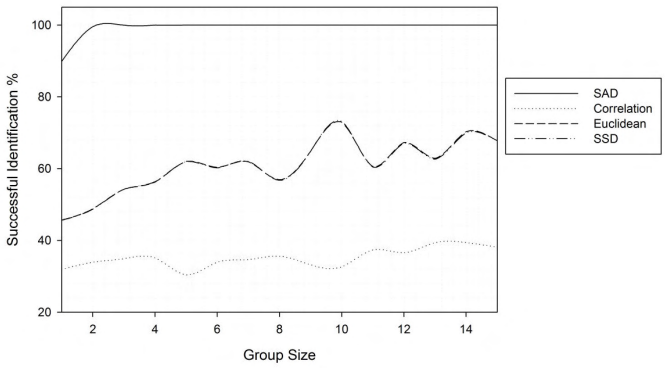

Fig. 8. Comparison of algorithm effectiveness versus the number of signatures averaged.

Each algorithm computes a single match value when executed on a library signature and live signature pair. The vehicle corresponding to the library signature that exhibits the best match with the live signature is selected. We evaluated the following simple algorithms

- **Sum of Absolute Differences (SAD)** – The total difference between the two signatures is calculated by adding the absolute value of differences between the 256 samples. The match with the smallest total difference is taken as best.
- **Sum of Squared Differences (SSD)** – The total difference between the two signatures is calculated by adding the square of differences between the 256 samples. The match with the smallest total difference is taken as best.
- **Euclidean Distance (ED)** – The total distance between the two signatures is calculated by taking the square root of the sum of squared differences. The match with the smallest total difference is taken as best.
- **Correlation (C)** – The correlation between the two signatures is calculated by taking the average pairwise product of the 256 samples. The match with the maximum correlation is taken as the best.

The results of this evaluation are depicted in Figure 8.

The vertical axis contains the percentage of correct matches, while the horizontal axis represents the varying number of raw signatures being averaged.

The algorithm with the best performance is clearly the SAD algorithm which exhibits almost perfect accuracy when at least 3 signatures are averaged. The SSD and ED algorithms exhibit moderate performance, and the Correlation algorithm performs poorly. This is significant for two reasons: (1) SAD is a simple and fast algorithm to execute on a microprocessor requiring only a handful of arithmetic operations for each sample, and (2) only having to average a small number of raw signatures to successfully differentiate vehicle classes means our radar can be utilized in a real-time scenario to perform the advanced control operations desired.

B. Live Target Identification

Utilizing the same basic setup described above, we evaluate the ability of the radar system to differentiate between live targets with the matching algorithm implemented on the XMOS microcontroller.

The test procedure begins by recording the background doppler signature which is then subtracted from subsequent measurements.

The library signature is recorded by averaging 30 raw signatures. It is this average signature that is used to identify the vehicle in subsequent measurements. This procedure was repeated for all three vehicles. Once the signatures for all the vehicles have been acquired, target identification can begin. (In a deployed radar system, however, these signatures will be stored in non-volatile memory on board the radar processor, or transmitted to the radar by the UAV's mission computer as needed).

The initial round of live target testing simulated a single target scenario (although the other targets were present, the rotors on the other vehicles were not moving). The radar system was pointed at each target, in turn, and the rotors on the respective target were brought to typical flight speeds. As anticipated by the earlier tests, the results with the SAD algorithm resulted in approximately 100 percent correct identification.

The second round of live target testing simulated multiple UAVs sharing the airspace in the region ahead of the host UAV. Two UAVs, in this case, the Lama v4 and the TRex were operated and the radar system was pointed at each vehicle in turn and a match computed. Despite the difference in vehicle size, the radar system correctly identified the target directly in front of the radar despite the "noise" generated by the other vehicle.

C. Flight Mounted on the Parrot

Finally, in order to demonstrate our claim that the radar system can be mounted on miniature UAVs, we fastened the radar onto a Parrot AR Drone. The prototype radar is 230g, the Parrot AR Drone without the protective fairing was able to hover with the radar onboard. It should be noted that the vehicle was operated 1600m above sea level. Furthermore the Parrot AR done is not designed to carry a payload, therefore by all metrics (flight time, wind resistance, forward velocity, etc...) the vehicle performance was reduced. However the tests were successful when considering the limitations of the host vehicle.

VII. CONCLUSIONS

In this paper we describe a novel radar system that is small enough to be mounted on a miniature UAV, and capable of both detecting and identifying other miniature UAVs. We describe the key hardware and software elements of the system, the results of our evaluation of various radar signature matching algorithms, and of utilizing the radar successfully in a laboratory environment to detect and identify real vehicles. While the response of a UAV to various threats is outside the scope of this paper, more information on this aspect of the system can be found in [19]. We envision this sensor as a key component of future miniature UAVs as they are integrated into the National Air Space, and take on non-military missions in many key application areas.

REFERENCES

[1] S. Research, "International military and civilian unmanned aerial vehicle survey," ASDReports, Tech. Rep., Nov. 2010.

[2] S. V. Lieven Dewitte, "M61 a1 vulcan: 20mm gatling gun system," Tech. Rep.

[3] Bombardier, "Learjet 40xr factsheet."

[4] E. A. S. Agency, "Bird strike damage & windshield bird strike final report," European Aviation Safety Agency, Tech. Rep.

[5] Introduction to TCASII, Version 7, U.S. Department of Transportation, Federal Aviation Administration, November 2000.

[6] Cessna, "Skyhawk model 172r: Specification & description," May 2010.

[7] J. Wellman, R. Silvious, "Doppler signature measurements of an mi-24 hind-d helicopter at 92ghz," United States Army Research Laboratory, Tech. Rep., July 1998.

[8] A. Cilliers and W. Nel, "Helicopter parameter extraction using joint time-frequency and tomographic techniques," in Radar, 2008 International Conference on, Sept. 2008, pp. 598 –603.

[9] N.-H. Lim, H. Myung, "A novel hybrid aipo-mom technique for jet engine modulation analysis," Progress In Electromagnetics Research, vol. 104, pp. 85–97, 2010.

[10] S. Yang, S. Yeh, S. Bor, S. Huang, and C. Hwang, "Electromagnetic backscattering from aircraft propeller blades," Magnetics, IEEE Transactions on, vol. 33, no. 2, pp. 1432 –1435, Mar. 1997.

[11] C. Rotander and H. Von Sydow, "Classification of helicopters by the l/n-quotient," in Radar 97 (Conf. Publ. No. 449), Oct. 1997, pp. 629 –633.

[12] V. Chen, W. Miceli, and B. Himed, "Micro-doppler analysis in isar - review and perspectives," in Radar Conference - Surveillance for a Safer World, 2009. RADAR. International, Oct. 2009, pp. 1 –6.

[13] E. Zaugg, D. Hudson, and D. Long, "The byu sar: A small, student-built sar for uav operation," in Geoscience and Remote Sensing Symposium, 2006. IGARSS 2006. IEEE International Conference on, Aug. 2006, pp. 411 –414.

[14] NanoSAR - Worlds Smallest SAR, imSAR.

[15] Roke, Miniature Radar Altimeter MRA Type 2 0.2-100m range, Roke Manor Research Limited.

[16] J. Volakis, "Chapter 14: Horn Antennas" in Antenna Engineering Handbook, 4th ed. McGraw-Hill Publications, 2007.

[17] L. Technology, LTC1864/LTC1865, Linear Technology Corporation.

[18] The Navigation and Control Technology Inside the AR.Drone Micro UAV. IFAC World Congress, 2011.

[19] UAV-Bourne X-Band Radar for MAV Collision Avoidance. SPIE Defense Security and Sensing, 2011.